Carbohydrate Polymers 89 (2012) 331–339

Contents lists available at SciVerse ScienceDirect

Carbohydrate Polymers

journal homepage: www.elsevier.com/locate/carbpol

Alterations in cell-wall glycosyl linkage structure of Arabidopsis *murus* mutants

Rachel A. Mertz[1], Anna T. Olek, Nicholas C. Carpita*

Department of Botany & Plant Pathology, Purdue University, 915 West State Street, West Lafayette, IN 47907-2054, United States

ARTICLE INFO

Article history:
Received 16 November 2011
Received in revised form 29 January 2012
Accepted 19 February 2012
Available online 28 March 2012

Keywords:
Arabidopsis thaliana
Mutants
Cell wall
Linkage structure
Principal Components Analysis

ABSTRACT

Methylation (glycosyl-linkage) analyses of the cell walls from Arabidopsis (*Arabidopsis thaliana* L., Heynh.) *murus* mutants revealed variations in the linkage structure compared to wild type. Linkage analyses revealed new features for mutations whose defective gene has not been identified. For example, the low-rhamnose *mur8* mutant also shows deficiencies in 4-GalA linkages. No change in the 2-Rha to 2,4-Rha ratio indicates the mutant had lower amounts of rhamnogalacturonan I, but no alteration in its fine structure. For all *mur* mutants, methylation analysis revealed that changes in other polysaccharides occur indirectly as a result of mutation. All mutants were resolved by Principal Components Analyses applied to normalized mole% values for the total set of linkage groups. The 'loadings' responsible for discrimination of mutant and wild type revealed variation in linkage groups otherwise difficult to discern and, in certain instances when the gene is known, resolved the specific deficiency from indirect effects altering other sugar linkage distributions.

1. Introduction

The plant cell wall is a rigid but dynamic structure of cellulose microfibrils tethered by a structurally diverse array of cross-linking glycans to form a strong, stable network, embedded in a pectin matrix and sometimes cross-linked further with structural proteins or phenolic substances (Carpita & Gibeaut, 1993; McCann & Roberts, 1991). An estimated 10% of a plant genome, about 2500 genes, is devoted to the synthesis, assembly, rearrangement, and disassembly of the cell wall (Penning et al., 2009; Yong et al., 2005). However, the precise function is known for only a small percentage of these genes. A valuable means to define function is to identify mutants deficient in a cell wall-related function. A screen of deficiencies in cell-wall monosaccharide distribution made in Arabidopsis led to discovery of 11 unique lines, named *mur1* through *mur11* (from the Latin *murus*, or wall), each with a deficiency in at least one monosaccharide (Reiter, Chapple, & Somerville, 1993, 1997). The degree of deficiency and number of monosaccharides affected varies between lines, with *mur1–mur3* null or deficient in Fuc, *mur4–mur6* deficient in Ara, *mur8* deficient in Rha, and *mur9–mur11* giving multiple deficiencies of varying severity.

We have classified the monosaccharide-deficient *mur* phenotypes by glycosyl-linkage analysis, a chemical derivatization technique employing separation and quantitation of partially methylated alditol acetates by gas–liquid chromatography/electron-impact mass spectrometry to determine the linkage composition of the sugars in the various complex polysaccharides. Glycosyl-linkage analysis determines the proportional contribution of sugar linkage groups, which in many instances are diagnostic of known polysaccharides from which they are derived. For example, the major cross-linking glycan, xyloglucan, is composed of a 4-linked glucan backbone with xylosyl residue added to the *O*-6 position of three of every four glucosyl residues in the backbone to give the 4,6-Glc (Carpita & Gibeaut, 1993). The *t*-Xyl residue in turn can have *t*-Gal residues added to the *O*-2 position to form 2-Xyl, and one of the *t*-Gal residues can be further extended with a *t*-Fuc residue at the *O*-2 position to form 2-Gal. Glucuronoarabinoxylans are less abundant but distinguishable by 4-linked xylosyl units of the backbone with *t*-Ara*f* at the *O*-2 or *O*-3 positions to form 2,4- and 3,4-Xyl branch points, as well as the *t*-GlcA residues at the *O*-2 positions. The major pectic polysaccharides are the homogalacturonan (HG) homopolymers of *O*-4 linked GalA residues, and rhamnogalacturonan I, a backbone of a disaccharide repeating unit of 2-Rha and 4-GalA with neutral sugar chains added to the Rha *O*-4 position. These chains are typically 5-linked and highly branched arabinans with *t*-Ara*f*, 2,5 and 3,5-Ara*f* branch point residues, 4-galactans, and type I galactans with *t*-Ara*f* residues at the *O*-3 position to for 3,4-Gal branch points. The degree of branching is estimated by the ratio of 2-Rha:2,4-Rha. During development, xylogalacturonans are synthesized where *t*-Xyl residues are added to the *O*-3 position of HGs to form 3,4-GalA residues characteristic of the modified polymer. A complex form of HG is rhamnogalacturonan II (RG II), which has a collection of unique monosaccharides and

* Corresponding author. Tel.: +1 765 494 4653; fax: +1 765 494 0363.
E-mail address: carpita@purdue.edu (N.C. Carpita).
[1] Present address: Department of Plant Biology, Cornell University, 412 Mann Library Building, Cornell University, Ithaca, NY 14853, United States.

0144-8617/$ – see front matter © 2012 Elsevier Ltd. All rights reserved.
doi:10.1016/j.carbpol.2012.02.044

glycosidic linkages, including apiose, which are not readily detected in the glycosyl-linkage analysis (Carpita & Gibeaut, 1993).

Conventional genetic mapping of some of these mutants has revealed the gene responsible for the deficiency. For example, *mur1*, a Fuc-null mutant, was traced to a defective GDP-α-D-Man-4,6-dehydratase that catalyzes the first step of the *de novo* synthesis of GDP-β-L-Fuc (Bonin et al., 1997; Reiter et al., 1993, 1997). *Mur2* and *mur3* were both characterized by about a 50% reduction in cell-wall Fuc, but neither has a visible shoot phenotype (Reiter et al., 1997). *MUR2* was defined by Vanzin et al. (2002) as encoding a xyloglucan-specific fucosyl transferase that adds a terminal fucose residue to form the characteristic α-L-Fuc*p*-(1 → 2)-β-D-Gal*p*-(1 → 2)-α-D-Xyl*p*-(1 → 6)-trisaccharide side chains of the xyloglucan backbone, and was allelic with the *AtFUT1* gene encoding the fucosyl transferase enzyme purified from pea epicotyls (Perrin et al., 1999).

Deducing the function of *MUR3* gene product was more challenging because of the confusion caused by the Fuc-deficient phenotype. When purified xyloglucans were digested with a *Trichoderma* endo-β-glucanase, analysis of the resultant oligomers by high-performance anion-exchange chromatography and electrospray tandem mass spectrometry revealed that the *MUR3* gene encodes a xyloglucan galactosyl transferase that specifically galactosylates the xylose closest to the reducing end of the oligomer (Madson et al., 2003). The Gal residue is essential for the attachment of Fuc, and its absence resulted in the Fuc deficiency in xyloglucan specifically. However, the abundance of Gal in several other polymers precluded identification of this mutant as a cell-wall Gal deficiency. Also, pleiotropic effects on sugar linkages can complicate efforts to characterize mutant phenotypes, particularly when the activity of the putative gene product has not been demonstrated.

Mur4 exhibits a 50% reduction in cell-wall Ara content. Because the wild-type Ara phenotype could be rescued by exogenous Ara to form UDP-Ara*p* via a salvage pathway, the deficiency was implicated in *de novo* nucleotide sugar biosynthesis (Reiter et al., 1997), and *MUR4* was subsequently found to encode Golgi-localized UDP-α-D-Xyl*p*:UDP-β-L-Ara*p* C4-epimerase by map-based cloning (Burget, Verma, Mølhøj, & Reiter, 2003). The *mur5* and *mur6* mutants also have lower cell-wall Ara content (Reiter et al., 1997), but the defective genes have not been identified. The wild-type levels of Ara are not rescued by exogenous Ara, indicating that the deficiency is downstream of the formation of UDP-β-L-Ara*p*. Likewise, the low-Rha deficiency of *mur8* has not yet been traced to a gene (Reiter et al., 1997). Of the seven *murus* mutants analyzed, only *mur1* and *mur8* have visible phenotypes when compared to wild type; *mur1* is characterized by a slightly shorter stature and a strongly reduced tensile strength of the floral stem (Reiter et al., 1993), and *mur8* is characterized by smaller rosettes with narrower leaves (Reiter et al., 1997).

Because the great number and abundance of each linkage group can make comparisons difficult, we used Principal Components Analysis (PCA) of the mol% of the major linkage structures of mutants and wild-type. For mutations in which the gene responsible for a sugar deficiency has been identified, our results indicate that PCA can resolve linkage deficiencies resulting directly from genetic mutations from those that may be attributed to pleiotropic effects.

2. Materials and methods

2.1. Growth of plant materials

Arabidopsis seeds of Col-0 and WS were obtained from a commercial source (Lehle seeds) and compared to stock sources from whence the mutants were derived. The "*murus*" mutants (*mur1-1*, *mur2-1*, *mur3-1*, *mur3-2*, *mur4*, *mur5*, *mur6*, and *mur8*) were obtained from Dr. Wolf-Dieter Reiter (University of Connecticut) as lines reselected for monosaccharide deficiency after six backcrosses with Col-0. Lines are grown out annually to preserve seed stocks.

Arabidopsis seeds were surface-sterilized with 70% (v/v) ethanol in water, then 10% Chlorox (6.25% $NaClO_2$) containing 0.05% Tween 20, and washed with sterile water. The seeds were incubated at 4 °C for three days. The seeds were sown in 100-plug trays containing a 3:1 (v/v) mixture of Metromix 510 and Vermiculite/Perlite, with 1 g L^{-1} Marathon insecticide, and 8 g L^{-1} Osmocote. The plants were grown for 45 days in a 16 h day/8 h night photoperiod, with a light intensity of 75 μmol photons m^{-2} s^{-1}. The plants were incubated for the last two days in darkness at 23 °C to lower starch content.

2.2. Isolation of cell walls

The rosette leaves of 45-d-old Arabidopsis plants were harvested into liquid nitrogen, then suspended in 50 mM Tris[HCl], pH 7.2, containing 1% SDS, and homogenized in a glass–glass motorized grinder (Kontes-Duall, Thomas Scientific, Swedesboro, NJ). The homogenates, with two rinses with Tris grinding buffer, were transferred to 15-mL Corning (Falcon) tubes and centrifuged at 2000 × *g* for 5 min. The supernatant liquids were discarded, and the pellets were suspended in 10 mL of fresh Tris grinding buffer and heated to 65 °C for 20 min to extract soluble proteins. Following centrifugation, the pellets were washed with warm (50 °C) water (3×), 50% (v/v) ethanol in water (3×), and water at ambient temperature (3×), with pellets isolated after each step. The isolated walls were suspended in water until further analysis.

2.3. Monosaccharide and linkage analyses

For each mutant and wild type, duplicate samples of isolated cell walls from four different populations of Arabidopsis plants were carboxyl-reduced with $NaBD_4$ after activation with a water-soluble carbodiimide, as described by Kim and Carpita (1992) and modified by Carpita and McCann (1996). A colorimetric assay for uronic acids in the presence of neutral sugars (Filisetti-Cozzi & Carpita, 1991) was used to confirm reduction of the carboxyl groups was 95% or greater. For each of the four sets, two samples of each were directed to monosaccharide and linkage analysis. Some of the glycosyl-linkage analyses were lost during processing, but leaving a minimum of six independent glycosyl-linkage analyses for each mutant sample. Uronosyl-reduced wall material (1–2 mg) was hydrolyzed in 1 mL of 2 M trifluoroacetic acid (TFA) at 120 °C for 90 min, and the supernatant was then evaporated in a stream of nitrogen.

The monosaccharides were reduced with $NaBH_4$ and alditol acetates were prepared as described previously (Gibeaut & Carpita, 1991). Derivatives were separated by gas–liquid chromatography (GLC) on a 0.25-mm × 30-m column of SP-2330 (Supelco, Bellefonte, PA). Temperature was held at 80 °C during injection, then ramped quickly to 170 °C at 25 °C min^{-1}, and then to 240 °C at 5 °C min^{-1} with a 10-min hold at the upper temperature. Helium flow was 1 mL min^{-1} with splitless injection. The electron impact mass spectrometry (EIMS) was performed with a Hewlett-Packard MSD at 70 eV and a source temperature of 250 °C. The proportion of 6,6-dideuteriogalactosyl was calculated using pairs of diagnostic fragments *m/z* 187/189, 217/219 and 289/291 according to the equation described in Kim and Carpita (1992) that accounts for spillover of ^{13}C.

For linkage analysis polysaccharides were per-*O*-methylated with Li^+ methylsulfinylmethanide, prepared by addition of *n*-butyllithium (Aldrich) to dry dimethyl sulfoxide (DMSO; Pierce

silylation grade) and methyl iodide (Aldrich) according to Gibeaut and Carpita (1991). The per-*O*-methylated polymers were recovered after addition of water to the mixture and partitioning into chloroform. The chloroform extracts were washed five times with a threefold excess of water each, and the chloroform was evaporated in a stream of nitrogen gas. The partly methylated polymers were hydrolyzed in 2 M TFA for 90 min at 120 °C, the TFA was evaporated in a stream of nitrogen gas, and the sugars were reduced with $NaBD_4$ and acetylated. The partly methylated alditol acetates were separated on the same column as the alditol acetates; after a hold at 80 °C for 1 min during injection and rapid ramping, the derivatives were separated in a temperature program of 160–210 °C at 2 °C per minute, then to 240 °C at 5 °C per minute, with a hold of 5 min at the upper temperature. All derivative structures were confirmed by electron-impact mass spectrometry (Carpita & Shea, 1989).

2.4. Data analysis

The values of mole% of each linkage group were used in Principal Components Analysis with WIN-DAS software (Kemsley, 1998) as described by McCann et al. (2007).

3. Results and discussion

3.1. Linkage analysis

The complex polysaccharides and glycoproteins of plants are synthesized primarily from seven neutral sugars and two uronic acids (Table 1). The seven *murus* mutants give the expected cell-wall monosaccharide deficiencies reported by Reiter et al. (1997), namely the Fuc-null *mur1*, Fuc-deficient *mur2* and *mur3*, the Ara-deficient *mur4*, *mur5*, and *mur6*, and the Rha-deficient *mur8* (Table 1). Although the defective genes of the first four *murus* mutants have been identified, glycosyl-linkage analyses have never been performed to fully characterize the impact of the mutations on the linkage structure to reveal the specific function of the gene and other changes in polysaccharide composition that might occur as a result of compensation for the deficiencies. For two of the mutant genes, *mur1* and *mur4*, their identities were traced to the nucleotide-sugar interconversion pathway (Bonin et al., 1997; Burget et al., 2003), and thus, a glycosyl-linkage analysis was deemed moot. For *mur2* and *mur3*, the specificity of deficiency was traced to alterations in xyloglucan structure, and electrospray ionization MS was employed instead of glycosyl-linkage analysis to deduce the fine structure of xyloglucan oligomers directly (Madson et al., 2003; Vanzin et al., 2002). In no study was the downstream impact of the mutation on synthesis or dynamics of other polysaccharide components of the cell wall investigated.

Glycosyl-linkage analysis gave expected variation in the linkage structure for those mutants where the defective gene was known (Table 2). The *t*-Fuc residues were undetectable in *mur1* and reduced to about one-half the proportion as in the Columbia-O wild-type in *mur2* and *mur3*. Attachment of *t*-Fuc residues to the subtending the *t*-Gal residue to the O-2 position results in 2-Gal, which is significantly reduced in *mur2* and *mur3*, but less so in *mur1*. In contrast to *mur2*, a defective xyloglucan-specific fucosyl transferase, *mur1* is defective in the *de novo* synthesis pathway, and some of the complement of *t*-Fuc is replaced by *t*-L-Gal, as a result of 3,5-epimerase activity in the absence of the defective 4,6-dehydratase (Reiter et al., 1993). As indicated by an increase in the ratio of 2-Rha:2,4-Rha compared to wild type, the *mur1* deficiency also resulted in a slight decrease in the degree of branching of RG I, as well as a decrease in the proportion of 5-Ara*f*:*t*-Ara*f* (Table 3). The *mur2* and *mur3* exhibited lower degrees branching of 5-arabinans compared to wild type, as observed by an increase in the ratio of *t*-Ara*f* to the 2,5- and 3,5-Ara*f* branch point residues. The *mur3* also had the lowest degree of RG I branching compared to wild and all other *mur* mutants. The *mur2* and *mur3* also exhibited a slightly lower ratio of the 5-Ara*f*:4-Gal pectic side-chains (Table 3).

For low-Ara *mur4*, *mur5*, and *mur6*, the deficiencies were generally shared by all the major Ara-linkages (Table 2). The ratios of 5-Ara*f*:*t*-Ara*f* were slightly higher in *mur5* and *mur6* compared to wild type, whereas *mur4* and *mur5* exhibited lower degrees of branching (Table 3). The percentages of *t*-Fuc residues are slightly elevated in all the low-Ara mutants. Small reductions in several Gal linkage groups, mainly *t*-Gal and *4*-Gal, were also observed in *mur6*, but not in *mur4* or *mur5*. In *mur4* and *mur6* concomitant changes in Ara and Gal residues resulted in significantly lower ratios of 5-Ara*f*:4-Gal compared to wild type (Table 3). All three low-arabinose mutants have slightly enhanced percentages of 4-GalA (Table 2).

The low-Rha *mur8* showed proportional deficiencies in all Rha linkage groups, including the *t*-Rha. The decrease in mole% Rha was matched by a decrease in the mole% of GalA (Table 1), particularly 4-GalA (Table 2), indicating a significant reduction in the amounts of RG I. Despite this deficiency the ratio of 2-Rha:2,4-Rha, indicating the degree of branching of RG I, remained about 2:1 (Table 3). However, significant increases in the 5-Ara*f*:*t*-Ara*f* ratio, decreases in arabinan branching, and increase in the 5-Ara*f*:4-Gal ratio were observed in *mur8* compared to wild type (Table 3).

3.2. Principal Components Analysis

The relationship between genotype and phenotype is not a simple one for mutants in cell wall-related genes – polysaccharides are secondary gene products subject to many modifications in the cell wall, and feedback mechanisms operate to compensate for compositional changes (McCann & Carpita, 2005). We established Fourier transform infrared (FTIR) microspectroscopy as a high throughput screen for cell wall phenotypes in populations of mutagenized plants and used Principal Components Analysis (PCA) and Linear Discriminant Analysis (LDA) to identify mutant spectrotypes (Chen et al., 1998). Here, we applied these algorithms to the linkage analyses, where, instead of baseline corrected, area-normalized IR spectral frequencies, we used the equivalent normalization of mole% values of each of the 37 linkage groups for six to eight independent samples for each mutant compared to Col-0. PCA is a data reduction method where the 37 linkage group variates of each individual of the populations of wild type and mutant are compared to the combined variate average, concentrating the variation in each individual into a single PC. These amounts derived are then subtracted from each individual, a new average is generated, and the algorithm iterated to give additional variation uncorrelated with PC1 (Kemsley, 1998). When the PC scores are plotted, clustering of members of the population is then observed. The 'loading', or the relative contribution of each variate to the score provides information on which linkages contribute most to the variation. The method is unbiased and independent of knowledge of the sugar deficiency. We expected this type of PCA to be a robust method to confirm statistically the differences observed between mutant and wild type, but more importantly we found PCA to have the added value to visualize the global differences in linkage structure among several mutants and wild type.

The drastic alterations in cell wall composition conferred by the *mur* mutations result in surprisingly few or no morphological effects in the rosette leaf anatomy (Reiter et al., 1997). The PCA revealed significant direct and indirect changes in other polysaccharide structures that might account for the compensatory changes in wall architecture. For example, when PCA is applied to *mur1* and wild type linkage distribution, the *t*-Fuc deficiency is observed in PC1. However, in addition, the increase PC1 of *mur1* also indicates an enhancement of linkages associated with the major

Table 1
Monosaccharide distributions of isolated cell walls of Col and *murus* mutants.

Sugar	Col	*mur1*	*mur2*	*mur3*	*mur4*	*mur5*	*mur6*	*mur8*
					mole%*			
Rha	10.1 ± 0.2	11.6 ± 0.9	10.7 ± 0.2	11.2 ± 0.5	11.1 ± 0.2	10.3 ± 0.5	11.8 ± 0.5	**6.9 ± 0.6**
Fuc	1.8 ± 0.2	**n.d.**	**0.9 ± 0.1**	**1.0 ± 0.0**	2.7 ± 0.1	2.3 ± 0.0	2.8 ± 0.1	2.4 ± 0.1
Ara	8.8 ± 0.4	6.9 ± 1.1	7.6 ± 0.1	6.7 ± 0.3	**4.4 ± 0.1**	**5.4 ± 0.3**	**5.0 ± 0.2**	11.2 ± 0.5
Xyl	13.5 ± 1.2	13.1 ± 0.2	12.9 ± 1.1	12.2 ± 0.4	16.3 ± 1.1	14.4 ± 0.4	13.6 ± 1.2	14.4 ± 0.9
Man	1.6 ± 0.2	2.0 ± 0.3	2.2 ± 0.3	1.8 ± 0.2	2.0 ± 0.3	2.4 ± 0.2	2.5 ± 0.2	2.7 ± 0.2
Gal	10.4 ± 0.8	9.7 ± 0.0	10.5 ± 1.5	10.5 ± 3.9	10.4 ± 0.8	10.7 ± 0.2	9.3 ± 0.3	10.3 ± 0.8
GalA	42.3 ± 3.6	45.6 ± 1.2	43.9 ± 3.2	45.5 ± 5.8	45.7 ± 1.7	44.6 ± 1.2	48.1 ± 1.0	36.9 ± 1.9
Glc	11.5 ± 1.2	10.8 ± 2.7	10.9 ± 0.0	10.6 ± 1.2	7.2 ± 0.0	9.7 ± 1.2	6.7 ± 6.9	15.0 ± 4.5
GlcA	0.3 ± 0.0	0.3 ± 0.0	0.4 ± 0.1	0.5 ± 0.2	0.2 ± 0.0	0.2 ± 0.0	0.2 ± 0.0	0.2 ± 0.0

* Values are the mean ± S.D. of six to eight samples. Carboxyl residues were activated with CMC and reduced with NaBD4 (Carpita & McCann, 1996) to their respective sugar; after acid hydrolysis, the sugars were converted to alditol acetates, separated by gas–liquid chromatography, and quantified as described (Gibeaut & Carpita, 1991). The proportions of uronic acid and neutral sugar were distinguished by EIMS as described (Kim & Carpita, 1992). n.d. = not detected; S.D. of ±0.0 denote values <±0.05.

pectins HG and RG I, but an RG I that is less branched and diminished in 5-linked α-arabinan and 4-linked β-galactan (Fig. 1). While the Col wild type plants exhibited little variation in PC1, they were widely variable in PC2, primarily in abundance of 4-linked xylans, a secondary wall polymer, and 3,4-GalA, a linkage diagnostic for xylogalacturonan (Fig. 1). The PC1 values account for 63% of the total variability in linkage structure, whereas PC2 accounts for an additional 15%.

Table 2
Comparison of sugar and linkage distribution of partially methylated alditol acetates.

Sugar and linkage	Col	*mur1*	*mur2*	*mur3*	*mur4*	*mur5*	*mur6*	*mur8*
					mole%*			
Fucose								
t-Fuc	1.8 ± 0.2	n.d.	0.9 ± 0.0	1.0 ± 0.5	2.7 ± 0.1	2.3 ± 0.0	2.8 ± 0.1	2.4 ± 0.0
Rhamnose								
t-Rha	1.0 ± 0.3	1.2 ± 0.3	1.2 ± 0.4	1.3 ± 0.4	0.8 ± 0.2	0.9 ± 0.4	1.0 ± 0.4	0.4 ± 0.1
2-Rha	5.8 ± 0.1	7.2 ± 0.2	5.9 ± 1.1	7.3 ± 0.4	7.0 ± 0.3	6.5 ± 0.6	7.2 ± 0.3	4.1 ± 0.2
2,3-Rha	0.2 ± 0.1	0.1 ± 0.0	0.2 ± 0.0	0.2 ± 0.1	0.2 ± 0.0	0.2 ± 0.1	0.2 ± 0.1	0.1 ± 0.1
2,4-Rha	3.1 ± 0.3	3.1 ± 0.2	3.4 ± 0.6	2.4 ± 0.4	3.1 ± 0.3	2.7 ± 0.5	3.4 ± 0.3	2.3 ± 0.0
Arabinose								
t-Araf	3.4 ± 0.3	2.9 ± 0.2	3.4 ± 0.9	2.7 ± 0.4	1.6 ± 0.4	1.7 ± 0.2	1.4 ± 0.3	3.3 ± 0.3
t-Arap	0.3 ± 0.1	0.4 ± 0.1	0.1 ± 0.0	0.2 ± 0.0	0.3 ± 0.1	0.5 ± 0.1	0.4 ± 0.1	0.3 ± 0.0
2-Araf	0.2 ± 0.0	0.1 ± 0.0	0.2 ± 0.0	0.2 ± 0.0	0.2 ± 0.0	0.3 ± 0.0	0.3 ± 0.0	0.1 ± 0.0
3-Araf	0.3 ± 0.0	0.3 ± 0.1	0.2 ± 0.1	0.2 ± 0.0	0.2 ± 0.1	0.1 ± 0.0	0.2 ± 0.1	0.2 ± 0.0
5-Araf	2.9 ± 0.3	1.8 ± 0.4	2.5 ± 0.3	2.4 ± 0.3	1.5 ± 0.3	2.1 ± 0.2	2.0 ± 0.3	4.9 ± 0.3
2,5-Araf	1.1 ± 0.3	1.1 ± 0.2	0.8 ± 0.2	0.7 ± 0.2	0.4 ± 0.1	0.4 ± 0.1	0.4 ± 0.2	1.5 ± 0.1
3,5-Araf	0.6 ± 0.1	0.3 ± 0.1	0.4 ± 0.1	0.3 ± 0.1	0.2 ± 0.1	0.3 ± 0.1	0.3 ± 0.1	0.9 ± 0.1
Xylose								
t-Xyl	7.0 ± 0.3	6.5 ± 0.7	5.8 ± 1.1	6.9 ± 0.3	8.7 ± 0.9	7.2 ± 0.4	6.6 ± 1.0	8.2 ± 0.6
2-Xyl	2.3 ± 0.1	2.3 ± 0.2	2.2 ± 0.4	1.7 ± 0.6	2.7 ± 0.4	2.7 ± 0.2	2.6 ± 0.4	2.9 ± 0.1
4-Xyl	2.9 ± 1.0	3.0 ± 0.4	3.7 ± 0.8	2.6 ± 0.5	3.8 ± 0.7	3.4 ± 0.2	3.4 ± 0.5	2.5 ± 0.1
2,4-Xyl	0.7 ± 0.2	0.7 ± 0.3	0.5 ± 0.2	0.5 ± 0.1	0.7 ± 0.3	0.6 ± 0.1	0.6 ± 0.2	0.4 ± 0.1
3,4-Xyl	0.6 ± 0.2	0.6 ± 0.2	0.7 ± 0.3	0.5 ± 0.1	0.4 ± 0.1	0.5 ± 0.1	0.4 ± 0.2	0.4 ± 0.1
Mannose								
4-Man	1.4 ± 0.1	1.5 ± 0.1	1.9 ± 0.4	1.4 ± 0.2	1.8 ± 0.2	2.0 ± 0.1	2.2 ± 0.2	2.4 ± 0.2
4,6-Man	0.2 ± 0.0	0.5 ± 0.1	0.3 ± 0.2	0.4 ± 0.1	0.2 ± 0.0	0.4 ± 0.1	0.3 ± 0.0	0.3 ± 0.1
Galactose								
t-Gal	4.2 ± 0.3	4.2 ± 0.3	4.1 ± 0.7	4.4 ± 0.6	4.1 ± 0.4	4.1 ± 0.4	3.4 ± 0.3	3.2 ± 0.2
2-Gal	1.7 ± 0.3	1.2 ± 0.4	0.5 ± 0.1	0.6 ± 0.4	1.5 ± 0.2	1.6 ± 0.2	1.4 ± 0.2	2.1 ± 0.2
3-Gal	0.4 ± 0.1	0.6 ± 0.1	0.4 ± 0.1	0.3 ± 0.1	0.2 ± 0.0	0.3 ± 0.1	0.3 ± 0.0	0.3 ± 0.0
4-Gal	1.6 ± 0.4	1.0 ± 0.1	1.6 ± 0.4	1.6 ± 0.3	1.5 ± 0.2	1.1 ± 0.4	1.3 ± 0.4	2.2 ± 0.2
6-Gal	0.8 ± 0.1	1.0 ± 0.3	1.4 ± 0.6	1.2 ± 0.4	1.4 ± 0.4	1.9 ± 0.3	1.1 ± 0.3	0.9 ± 0.2
2,4-Gal	1.0 ± 0.1	0.9 ± 0.2	1.1 ± 0.3	1.3 ± 0.2	1.1 ± 0.2	1.1 ± 0.4	1.2 ± 0.2	1.2 ± 0.3
3,4-Gal	0.4 ± 0.2	0.6 ± 0.5	0.9 ± 0.7	0.7 ± 0.4	0.3 ± 0.0	0.3 ± 0.1	0.2 ± 0.1	0.2 ± 0.0
3,6-Gal	0.3 ± 0.0	0.2 ± 0.1	0.5 ± 0.2	0.4 ± 0.1	0.3 ± 0.0	0.3 ± 0.1	0.4 ± 0.1	0.2 ± 0.0
Galacturonic acid								
t-GalA	0.9 ± 0.1	1.3 ± 0.2	0.8 ± 0.2	4.0 ± 1.6	0.9 ± 0.2	0.8 ± 0.5	1.2 ± 0.2	0.6 ± 0.1
4-GalA	31.0 ± 1.7	34.0 ± 1.2	32.8 ± 3.2	31.6 ± 3.3	34.7 ± 1.3	35.5 ± 0.7	37.1 ± 0.9	27.3 ± 1.0
2,4-GalA	1.3 ± 0.3	1.6 ± 0.3	1.5 ± 0.3	1.5 ± 0.3	1.1 ± 0.2	1.2 ± 0.2	1.2 ± 0.1	0.7 ± 0.2
3,4-Gal A	9.1 ± 1.7	8.7 ± 0.3	8.8 ± 0.4	8.4 ± 0.9	10.0 ± 0.5	3.5 ± 1.1	8.6 ± 0.8	8.3 ± 0.4
Glucose								
t-Glc	0.1 ± 0.0	0.1 ± 0.0	0.2 ± 0.1	0.1 ± 0.1	0.1 ± 0.0	0.1 ± 0.0	0.1 ± 0.0	0.1 ± 0.0
4-Glc	6.5 ± 0.7	6.1 ± 0.3	6.0 ± 1.1	5.9 ± 1.3	4.3 ± 0.2	5.9 ± 0.7	3.9 ± 0.1	9.2 ± 0.9
2,4-Glc	0.1 ± 0.1	0.1 ± 0.1	0.2 ± 0.1	0.2 ± 0.1	tr	tr	0.1 ± 0.0	tr
3,4-Glc	0.9 ± 0.1	0.9 ± 0.1	0.9 ± 0.1	0.7 ± 0.2	0.6 ± 0.0	0.5 ± 0.1	0.6 ± 0.1	0.9 ± 0.1
4,6-Glc	3.9 ± 0.4	3.6 ± 0.2	3.6 ± 0.6	3.7 ± 1.2	2.2 ± 0.2	3.2 ± 0.5	2.0 ± 0.2	4.8 ± 0.4
Glucuronic acid								
t-GlcA	0.3 ± 0.0	0.3 ± 0.0	0.4 ± 0.1	0.5 ± 0.2	0.2 ± 0.0	0.2 ± 0.0	0.2 ± 0.0	0.2 ± 0.0

* Values are the mean ± S.D. of six to eight samples. Carboxyl-reduced wall preparations were permethylated, reduced and acetylated as described (Gibeaut & Carpita, 1991). Linkage groups were established from GLC-EIMS as described (Carpita & Shea, 1989). The proportions of uronic acid and neutral sugar in the linkage groups were distinguished by EIMS as described (Carpita & Shea, 1989). tr = trace amounts less than 0.05%; n.d. = not detected; S.D. of ±0.0 denote values <±0.05.

Table 3
Ratios of linkage groups to reveal relative branching, and the proportions and types of pectic side-chains.

Ratio	Col	*mur1*	*mur2*	*mur3*	*mur4*	*mur5*	*mur6*	*mur8*
					Ratio			
2-Rha:2,4-Rha	1.9:1	2.3:1	1.7:1	3.0:1	2.3:1	2.4:1	2.1:1	1.9:1
5-Araf:t-Araf	0.9:1	0.6:1	0.7:1	0.9:1	0.9:1	1.2:1	1.4:1	1.5:1
t-Araf:branched	2.0:1	2.1:1	2.8:1	2.7:1	2.7:1	2.4:1	2.0:1	1.4:1
5-Araf:4-Gal	1.8:1	1.8:1	1.6:1	1.5:1	1.0:1	1.9:1	1.5:1	2.2:1

Values in Table 2 are used in calculating these ratios.

For *mur2*, for which a fucose deficiency was traced to a defect xyloglucan specific transferase (Vanzin et al., 2002), PC1 accounted for only 55% of the variance, with PC2 contributing only an additional 18%. However, it is PC2 that separates mutant from wild type, characterized by higher abundance in xyloglucan-diagnostic *t*-Fuc, *t*-Xyl and 2-Gal in wild type (Supplementary Fig. 1). Similarly, the fucose-deficient *mur3* mutants are resolved from wild type by an enrichment in PC2, which accounts for 34% of the variation. In this instance, increases in PC2 correlate with specific deficiencies in *t*-Fuc and 2-Gal (Fig. 2); like *mur2* these are residues that are diagnostic of the expected alterations in xyloglucan structure. The *mur3* mutants exhibit variability in PC1, primarily a result of variation in HG and relatively unbranched RG I, but further alterations specific to *mur3* include an increase in RG I with lesser degrees of

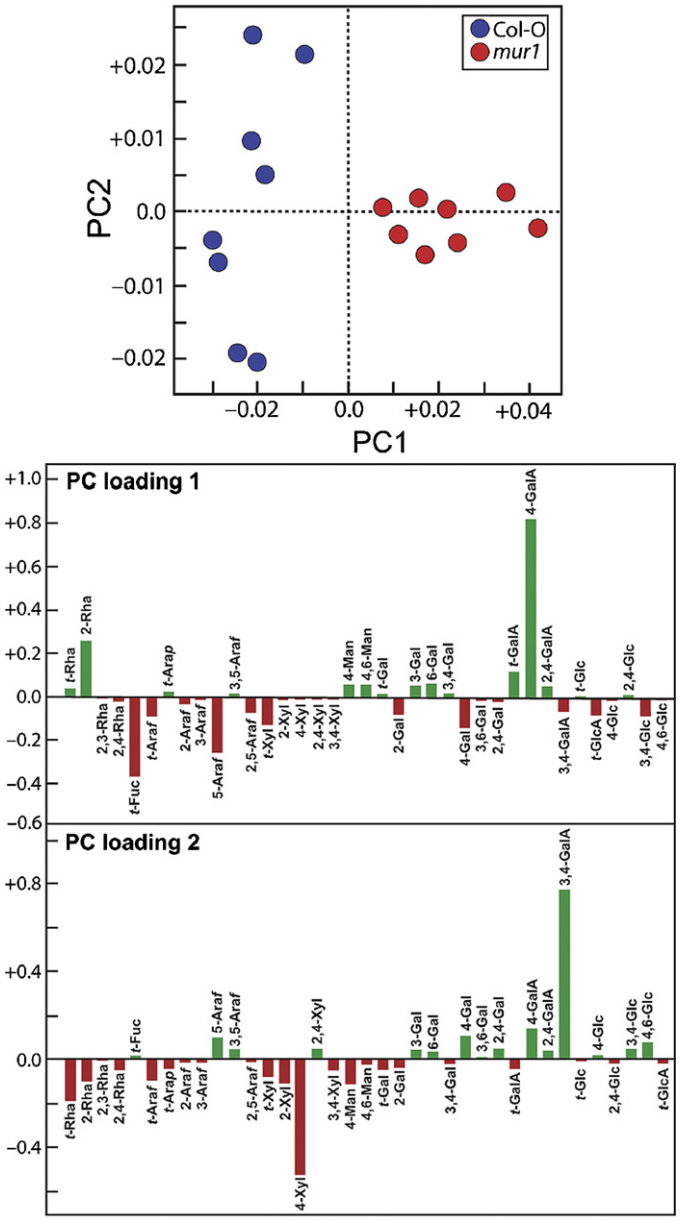

Fig. 1. Principal Components Analysis of the linkage structure of wild type and the Fuc-null *mur1*. PC1 and PC2 account for 63.0% and 14.8% of the variance, respectively. Mutant and wild type are separated primarily by linkage distributions contributing to PC1.

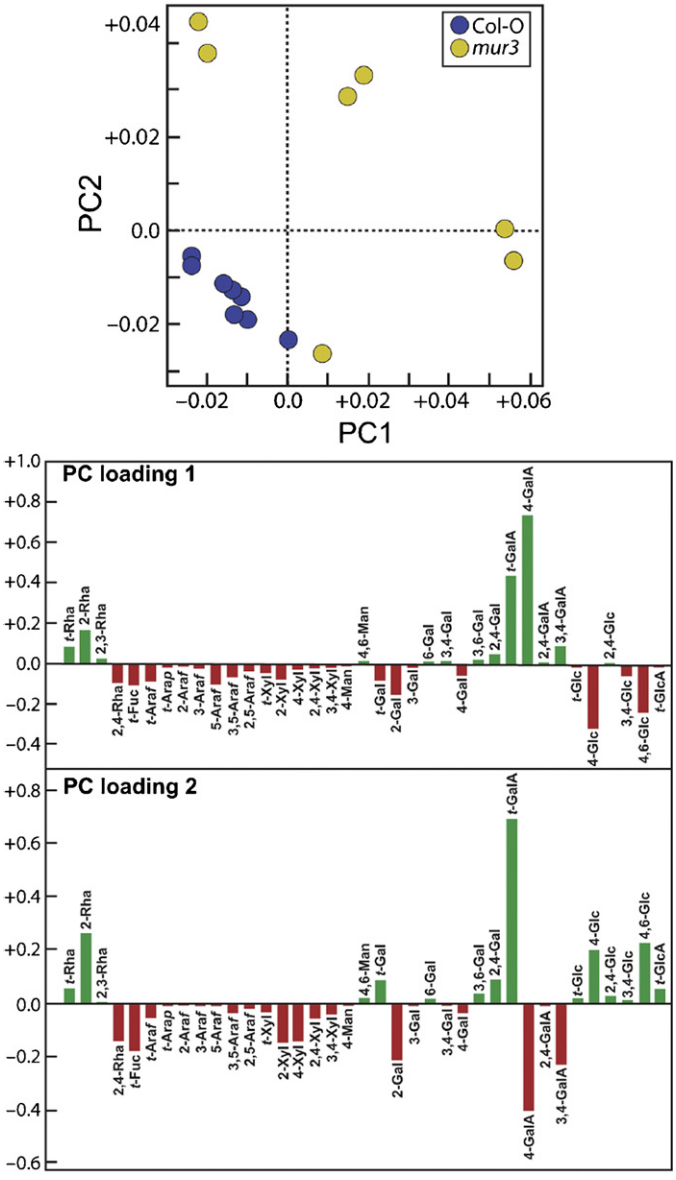

Fig. 2. Principal Components Analysis of the linkage structure of wild type and the Fuc-deficient *mur3*. PC1 and PC2 account for 41.3% and 34.1% of the variance, respectively. Mutant and wild type are separated primarily by linkage distributions contributing to PC2.

substitution with both α-arabinan and β-galactan (Fig. 2). A curious enhancement of *t*-GalA residues relative to 4-GalA residues indicates a possible fragmentation of HG.

These are interesting findings in light of the biochemical and biophysical phenotypes associated with *mur1*, *mur2*, and *mur3*. When mur1 was discovered as a fucose null, the conclusion, based on a brittleness of the floral stem, was that the fucosylated side-chain of xyloglucan was essential for wall tensile strength (Reiter et al., 1993). Subsequent work showed that lack of fucose in the side-group structure of RG II compromised this pectin's ability to bind to boron and contribute to cross-linking structure. Growing *mur1* plants in elevated boron rescued the wild-type phenotype (O'Neill, Eberhard, Albersheim, & Darvill, 2000), and the near elimination of the fucosylated xyloglucan side-chain specifically in *mur2* and *mur3* did not compromise tensile strength of the floral stem (Madson et al., 2003; Vanzin et al., 2002). Mechanical responses of *mur1* and *mur3* hypocotyls indicated that both xyloglucan and RG II contribute to wall tensile strength (Ryden et al., 2003). These data underscore the value of PCA to reveal changes in linkage structure beyond the specific deficiency.

The Ara-deficient *mur4* mutants are separated from wild type primarily by PC1, with each exhibiting variability in amounts of PC2 (Supplementary Fig. 2). While the PC1, which accounts for 70% of the variability, demonstrates the Ara deficiencies in both *t*-Ara*f*, 5-Ara*f*, and all Ara linked and branch-point residues, and increase in HG and RG I is also observed. Differences among mutants can also be revealed by PCA in three-way and four-way comparisons. For example, when we compared the three mutants with the largest monosaccharide deficiencies, the Fuc-null *mur1*, the Ara-deficient *mur4*, and the Rha-deficient *mur8*, with Col-0 wild type, and were able to resolve all three mutants from wild type completely with only two PCs (Fig. 3). The *mur8* was deficient in PC1 compared to wild type, whereas both *mur1* and *mur4* were equally enriched. An increase in PC1, although dominated by 4-GalA at the expense of most Glc linkages, was accounted for by increased proportions of Rha linkages and decreases in *t*-Fuc and all arabinofuranosyl linkages. Although similar in PC1 profile, *mur1* and *mur4* were completely resolved by PC2, largely dominated by increased *t*-Fuc, *t*-Xyl and xylosyl linkages, and 3,4-GalA (Fig. 3). PC1 accounted for about 69% of the variance, with PC2 adding 15% for a total of 84%. Increases in PC2 are also correlated with marked decreases in Ara, GalA and Glc linkages. These findings are consistent with the known deficiencies of *mur1* and *mur4*, and give fresh insight to the *mur8*, for which the defective gene is still not known. While the relatively low amounts of Rha and GalA linkages are expected, the relative increases in *t*-Fuc, 2-Gal, 2-Xyl, and 4- and 4,6-Glc, are indicative of higher relative amounts of xyloglucan; all 5-linked and branched arabinan linkages were increased as well, indicating possible compensatory increases in these typical side-chains of RG I.

The Fuc-deficient *mur2* and *mur3* mutants alter xyloglucan structure specifically, but the glycosyl-linkage analysis reveals only subtle differences in linkage structure (Supplementary Fig. 3). Only *mur3* showed significant increases in PC1, but PC2 variability was similar for mutant and wild type. Because of the subtle differences in linkage structure between these two mutants and wild type, PC1 accounted for only 45% of the variance, with PC2 adding 26%. An increase in PC1 indicates increases in Rha linkages and *t*-GalA, as well as *t*-Xyl, but decreases in Ara and Gal linkages, 2-Xyl from xyloglucan and all linked and branch xylans. The increase in *t*-Xyl at the expense of 2-Xyl and 2-Gal is consistent with the increase in galactosylation of the middle Xyl upon failure to galactosylate the first xylosyl residue of the Arabidopsis xyloglucan (Madson et al., 2003).

The Ara-deficient *mur4*, *mur5*, and *mur6* are all resolved from Col-0 and each other by the first two PCs, which account for 63% and 12% of the variance, respectively (Fig. 4). The *mur6* was most enriched in PC1, characterized primarily by high abundance of the 4-GalA from HG and small amounts of RG I, indicated by Rha linkages. Deficiencies in the linked and branched arabinans and several glucosyl linkages are also indicated. The *mur4* and *mur5* are relatively enriched in PC1 compared to wild type, but equally enriched in PC2 compared to wild type and *mur6* (Fig. 4). The loading of PC2 is characterized also by decreases specifically in the Ara linkages and branch-point residues, the exceptions being *t*-Ara*p* and 2-Ara*f*. The PC2 loading also reveals increases in *t*-Xyl and 3,4-GalA, indicative of xylogalacturonan, and a positive 2-Rha paired with a negative 2,4-Rha indicates an RG I with a lower degree of branching. Both PC1 and PC2 loadings show that all *mur* mutants have less glucan than wild type. Although *mur4* has been characterized for the

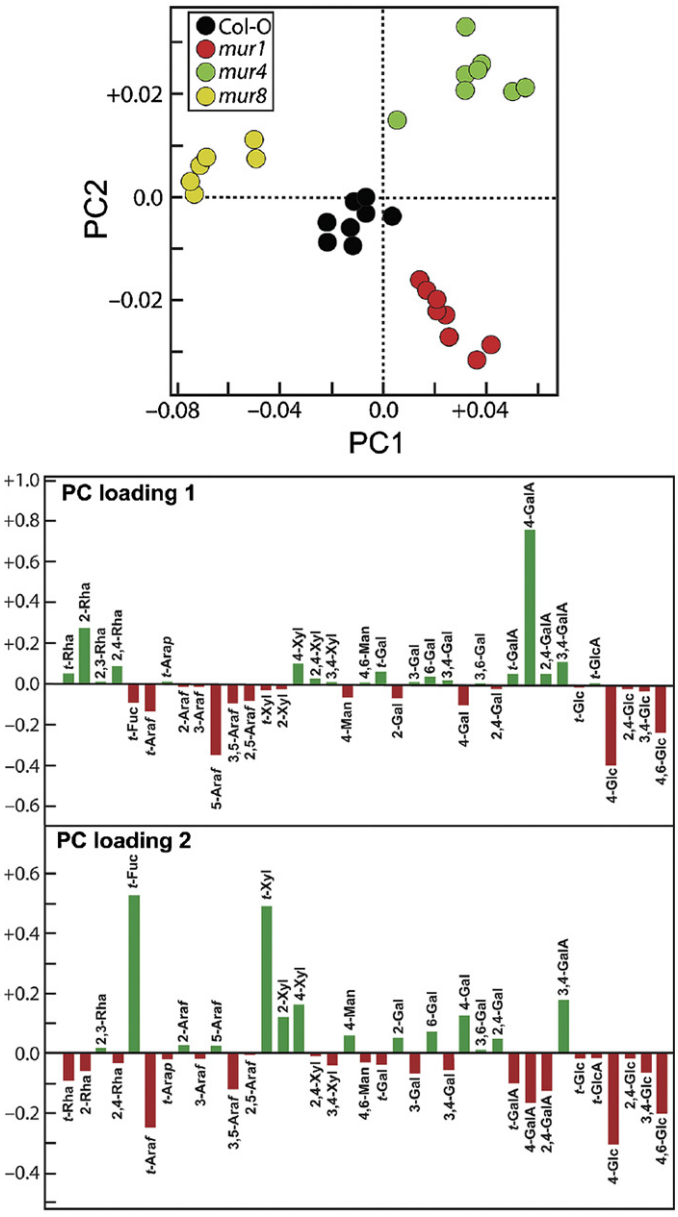

Fig. 3. Principal Components Analysis of the linkage structure of wild type and the Fuc-null *mur1*, the Ara-deficient *mur4*, and the Rha-deficient *mur8*. PC1 and PC2 account for 69.3% and 15.0% of the variance, respectively. The *mur1* and *mur4* are widely separately from *mur8* by PC1, primarily by scores for deficiencies in Ara*f* linkages and high proportions of Rha and GalA linkages. The *mur1* is separated from *mur4* by PC2, which accounts for higher abundance of primarily *t*-Fuc and *t*-Xyl residues.

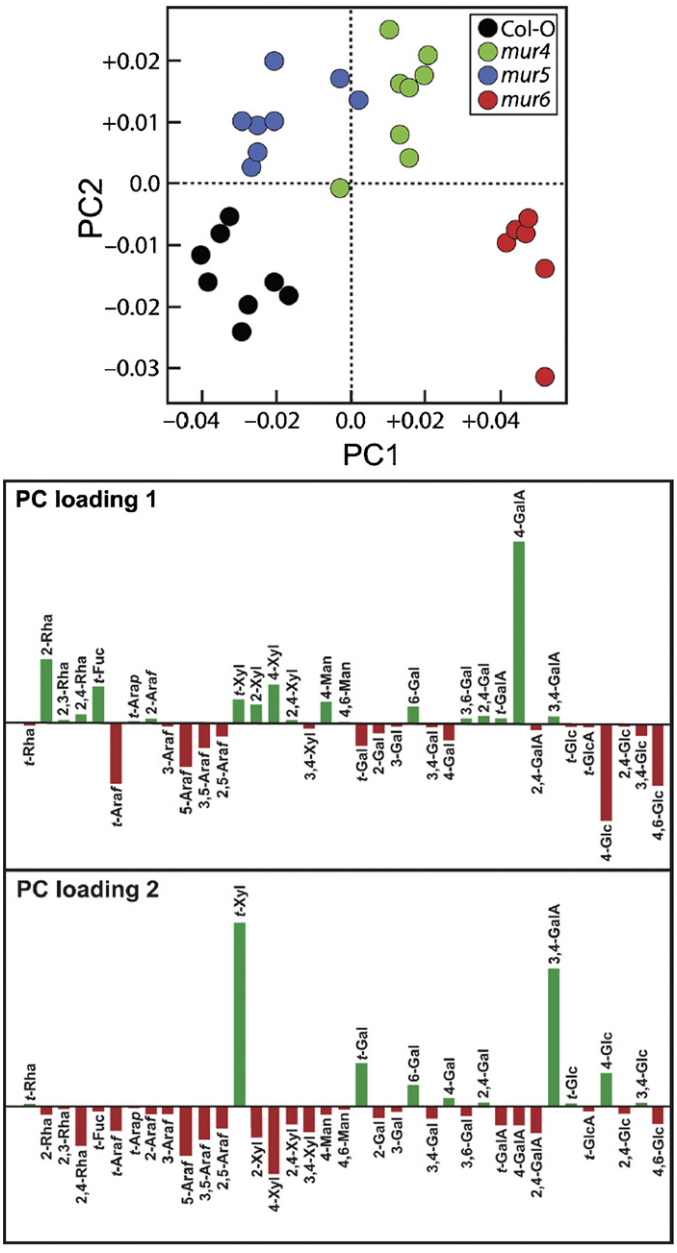

Fig. 4. Principal Components Analysis of the linkage structure of wild type and the Ara-deficient *mur4*, *mur5*, and *mur6*. PC1 and PC2 account for 63.1% and 11.9% of the variance, respectively. Mutants and wild type are separated primarily by PC1 which scores for Ara deficiencies and higher abundance of HG and RG I, as well as linkages associated with xylans. The *mur4* and *mur5* are more closely related in structure with respect to PC2, showing again added Ara deficiencies, but differences in pectin structure from PC1.

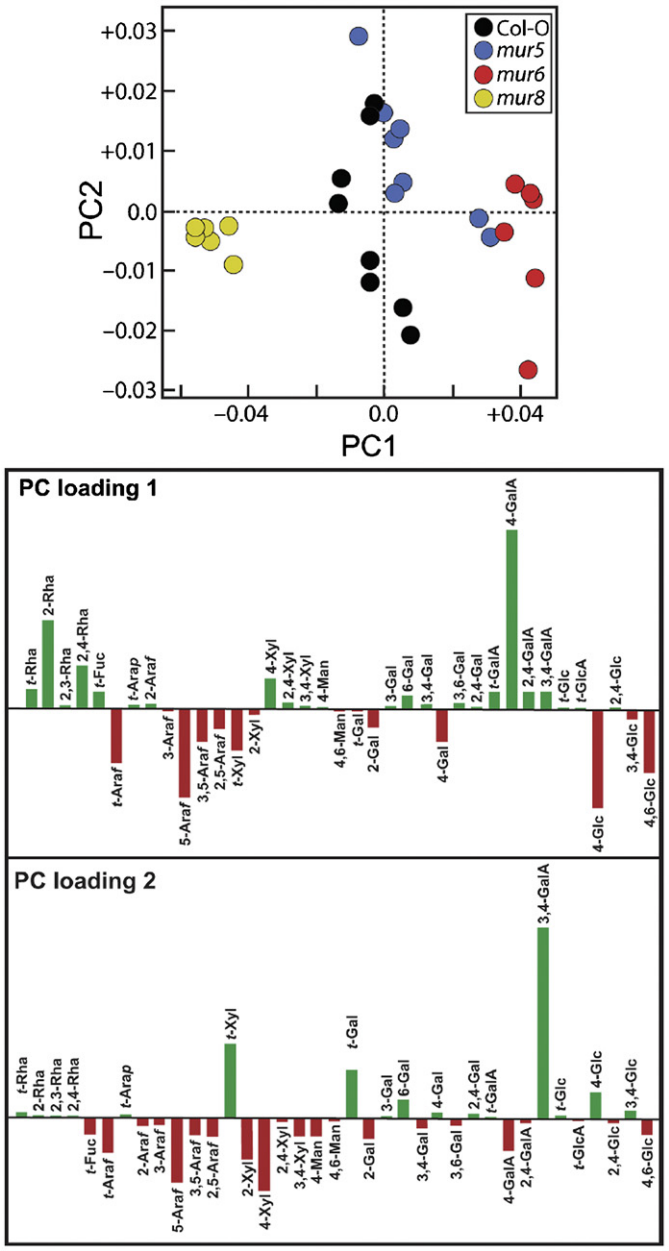

Fig. 5. Principal Components Analysis of the linkage structure of wild type and the Ara-deficient *mur5* and *mur6* with the Rha-deficient *mur8*. PC1 and PC2 account for 88% and 5.8% of the variance, respectively. The *mur8* is deficient in PC1, which scores for high abundance of Rha and GalA linkages coupled with deficiencies in Ara*f* linkages.

defect in the C-4 epimerase that interconverts UDP-Xyl*p* and UDP-Ara*p* (Burget et al., 2003), *mur4* and *mur5* share similar features in linkage analysis, even though both *mur5* and *mur6* have defects in genes downstream of *mur4*, given the inability of exogenous Ara to rescue the Ara-deficient phenotype to wild type levels (Reiter et al., 1997). The deficiencies in Ara*f* residues and in *mur5* and *mur6* loadings were not strongly associated with a specific linkage group (Fig. 4).

Because of some potential pleiotropic effects on HG and RG I found in the Ara-deficient *mur5* and *mur6*, we performed the PCA including the Rha-deficient *mur8*. The *mur6* is most abundant in PC1, *mur8* the least, and *mur5* and wild type intermediate (Fig. 5). Increases in PC1, which alone accounts for 88% of the variance, are associated with increased HG and RG I linkages and deficiencies in 5-linked and branched arabinans. The *mur5* and wild type are resolved in PC2, with *mur5* enriched in RG I and 3,4-GalA instead of the 4-GalA of unsubstituted HG in addition to deficiencies in all Ara linkages. Also, the relatively higher abundance of *t*-Xyl and *t*-Gal linkages in *mur5* contributed to distinguishing it from wild type (Fig. 5).

4. Conclusions

Linkage analyses have substantially extended the interpretations of *murus* mutants beyond the recognition of monosaccharide deficiencies. These analyses are consistent with the defective enzymatic activity in the four instances where the gene is known and

have given insight to the possible defects in mutants for which the genes have not yet been identified. Principal Components Analysis is an effective method to validate that the subtle alterations in linkage structure between mutant and wild type are not a result of sample variation. In addition to indicating the primary linkage differences that result from the monosaccharide deficiency, downstream impacts on cell wall structure with respect to adjustments in pectin, xyloglucan, and arabinoxylan structures are also possible. The PCA is a robust method to visualize and distinguish total linkage composition differences between wild type and mutant.

The limitations of PCA must also be noted. PCA is not robust in classification when many classes are included and when wall composition or architecture distinguishes each class in a different way. If large sets of cell wall phenotypes are to be compared, e.g. on a genome-wide scale, more robust classification tools, such as Artificial Neural Networks, are required to extract multivariate data from large numbers of observations and large numbers of potential classes of observations within a data set (McCann et al., 2007). The neural network reports both on class assignment (percent correct classification) and the probability of membership of each class. However, while neural networks are very good at clustering populations based on similarities, the basis of those separations remain obscure.

PCA is applied to other kinds of phenotype analyses where large numbers of variates can be quantized, such as the use of NMR in metabolite profiling in marker-assisted selection for disease resistance (Browne & Brindle, 2007). An application of PCA would prove useful in analysis of large glycomics arrays, where 180 plant glycan-directed monoclonal antibodies form a panel identify carbohydrate epitopes in several fractions of plant cell walls (Pattathil et al., 2010). Classification of the broad range of mutants must account for genes that function only during certain developmental stages. For example, changes in the degree of branching of RG I are associated with the appearance and disappearance of neutral side groups in a cell- and developmental stage-specific manner (Ulvskov et al., 2005; Vincken et al., 2003), and RG I polymers are typically highly substituted with branched and unbranched forms of α-L-arabinans enriched in meristematic cells are replaced by forms of RG I enriched in the β-galactans (Bush, Marry, Huxam, Jarvis, & McCann, 2001). Loss of β-galactans occurs during maturation of tomato (*Solanum lycopersicum*) ripening (Gross & Sams, 1984), and loss of the highly branched α-arabinans, but not the (1 → 5)-α-L-arabinans, and debranching of an RG I are associated with the loss of firm texture in apple during storage (Peña & Carpita, 2004). The RG I of Arabidopsis mucilage is virtually unbranched at maturity (Penfield, Meissner, Shoue, Carpita, & Bevan, 2001), and glycosyl-linkage analysis has be useful to characterize mutations that result in impaired hydrolases that normally trim the galactan and arabinan side-chains (Arsovski et al., 2009; Dean et al., 2007). In some instances composites of polysaccharides, such as those of RG I and arabinoxylans of flax mucilage, are made in which each polysaccharide is drastically altered from their classic forms to fulfill a specialized function (Naran, Chen, & Carpita, 2008). Thus, PCA provides researchers with an enhanced evaluation tool for examining changes in cell wall composition that arise not only from mutations or natural variation, but also those that occur during development or in response to biotic and abiotic stresses.

Acknowledgments

We thank Dr. Maureen McCann (Purdue University) for advice on PCA protocols and review of the manuscript. The methylation analyses were supported by the National Science Foundation Plant Genome Research and REU Programs (Grant no. DBI-0217552 to N.C.C.), and the application of PCA to analyses was supported as part of the Center for Direct Catalytic Conversion of Biomass to Biofuels (C3Bio), an Energy Frontier Research Center funded by the U.S. Department of Energy, Office of Science, Office of Basic Energy Sciences under Award Number DE-SC0000997.

Appendix A. Supplementary data

Supplementary data associated with this article can be found, in the online version, at doi:10.1016/j.carbpol.2012.02.044.

References

Arsovski, A. A., Popma, T. M., Haughn, G. W., Carpita, N. C., McCann, M. C., & Western, T. L. (2009). AtBXL1 encodes a bifunctional β-D-xylosidase/α-L-arabinofuranosidase required for pectic arabinan modification in Arabidopsis mucilage secretory cells. *Plant Physiology*, *150*, 1219–1234.

Bonin, C. P. I., Potter, I. G. F., Vanzin, G. F., & Reiter, W.-D. (1997). The *MUR1* gene of *Arabidopsis thaliana* encodes an isoform of GDP-D-mannose-4,6-dehydratase, catalyzing the first step in the *de novo* synthesis of GDP-L-fucose. *Proceedings of the National Academy of Sciences of the United States of America*, *95*, 2085–2090.

Browne, R. A., & Brindle, K. M. (2007). ^{1}H-NMR-based metabolite profiling as a potential selection tool for breeding passive resistance against Fusarium head blight (FHB) in wheat. *Molecular Plant Pathology*, *8*, 401–410.

Burget, E. G., Verma, R., Mølhøj, M., & Reiter, W-D. (2003). The biosynthesis of L-arabinose in plants: Molecular cloning and characterization of a Golgi-localized UDP-D-xylose 4-epimerase encoded by the *MUR4* gene of Arabidopsis. *Plant Cell*, *15*, 523–531.

Bush, M. S., Marry, M., Huxam, I. M., Jarvis, M. C., & McCann, M. C. (2001). Developmental regulation of pectic epitopes during potato tuberization. *Planta*, *213*, 869–880.

Carpita, N. C., & Gibeaut, D. M. (1993). Structural models of primary cell walls in flowering plants: Consistency of molecular structure with the physical properties of the walls during growth. *Plant Journal*, *3*, 1–30.

Carpita, N. C., & McCann, M. C. (1996). Some new methods to study plant polyuronic acids and their esters. In R. Townsend, & A. Hotchkiss (Eds.), *Progress in glycobiology* (pp. 595–611). New York: Marcell Dekker.

Carpita, N. C., & Shea, E. M. (1989). Linkage structure of carbohydrates by gas chromatography–mass spectrometry (GC–MS) of partially methylated alditol acetates. In C. J. Biermann, & G. D. McGinnis (Eds.), *Analysis of carbohydrates by GLC and MS* (pp. 155–216). Boca Raton, FL: CRC Press.

Chen, L-M., Carpita, N. C., Reiter, W-D., Wilson, R. W., Jeffries, C., & McCann, M. C. (1998). A rapid method to screen for cell wall mutants using discriminant analysis of Fourier transform infrared spectra. *Plant Journal*, *16*, 385–392.

Dean, G. H., Zheng, H., Tewari, J., Huang, J., Young, D. S., Hwang, Y. T., et al. (2007). The Arabidopsis *MUM2* gene encodes a β-galactosidase required for the production of seed coat mucilage with correct hydration properties. *Plant Cell*, *19*, 4007–4021.

Filisetti-Cozzi, T. M. C. C., & Carpita, N. C. (1991). Measurement of uronic acids interference from neutral sugars. *Analytical Biochemistry*, *197*, 157–162.

Gibeaut, D. M., & Carpita, N. C. (1991). Tracing cell-wall biogenesis in intact cells and plants. Selective turnover and alteration of soluble and cell-wall polysaccharides in grasses. *Plant Physiology*, *97*, 551–561.

Gross, K. C., & Sams, C. E. (1984). Changes in cell wall neutral sugar composition during fruit ripening: A species survey. *Phytochemistry*, *23*, 2457–2461.

Kemsley, E. K. (1998). *Discriminant analysis of spectroscopic data*. Chichester, UK: John Wiley and Sons.

Kim, J.-B., & Carpita, N. C. (1992). Changes in esterification of the uronic acid groups of cell wall polysaccharides during elongation of maize coleoptiles. *Plant Physiology*, *98*, 646–653.

Madson, M., Dunand, C., Verma, R., Vanzin, G. F., Caplan, J., Li, X., et al. (2003). Xyloglucan galactosyltransferase a plant enzyme in cell wall biogenesis homologous to animal exostosins. *Plant Cell*, *15*, 1662–1670.

McCann, M. C., & Carpita, N. C. (2005). Looking for invisible phenotypes in cell-wall mutants of *Arabidopsis thaliana*. *Plant Biosystems*, *139*, 80–83.

McCann, M. C., & Roberts, K. (1991). Architecture of the primary cell wall. In C. W. Lloyd (Ed.), *The cytoskeletal basis of plant growth and form* (pp. 109–129). New York: Academic Press.

McCann, M. C., Defernez, M., Urbanowicz, B. R., Tewari, J. C., Langewisch, T., Olek, A., et al. (2007). Neural network analyses of infrared spectra for classifying cell wall architectures. *Plant Physiology*, *143*, 1314–1326.

Naran, R., Chen, G., & Carpita, N. C. (2008). Novel rhamnogalacturonan I and arabinoxylan polysaccharides of flax seed mucilage. *Plant Physiology*, *148*, 132–141.

O'Neill, M. A., Eberhard, S., Albersheim, P., & Darvill, A. G. (2000). Requirement of borate cross-linking of cell wall rhamnogalacturonan II for Arabidopsis growth. *Science*, *294*, 846–849.

Pattathil, S., Avci, U., Baldwin, D., Swennes, A. G., McGill, J. A., Popper, Z., et al. (2010). A comprehensive toolkit of plant cell wall glycan-dircted monoclonal antibodies. *Plant Physiology*, *153*, 514–525.

Peña, M. J., & Carpita, N. C. (2004). Loss of highly branched arabinans and debranching of rhamnogalacturonan I accompany loss of firm texture and cell separation during prolonged storage of apples. *Plant Physiology*, *135*, 1305–1313.

Penfield, S., Meissner, R. C., Shoue, D. A., Carpita, N. C., & Bevan, M. W. (2001). MYB61 is required for mucilage deposition and extrusion in the Arabidopsis seed coat. *Plant Cell*, *13*, 2777–2791.

Penning, B. W., Hunter, C. T., Tayengwa, R., Evelund, A. L., Dugard, C. K., Olek, A. T., et al. (2009). Genetic resources for maize cell wall biology. *Plant Physiology*, *151*, 1703–1728.

Perrin, R. M., DeRocher, A. E., Bar-Peled, M., Zeng, W., Norambuena, L., Orellana, A., et al. (1999). Xyloglucan fucosyltransferase an enzyme involved in plant cell wall biosynthesis. *Science*, *284*, 1976–1979.

Reiter, W.-D., Chapple, C. C. S., & Somerville, C. R. (1993). Altered growth and cell walls in a fucose-deficient mutant of Arabidopsis. *Science*, *261*, 1032–1035.

Reiter, W.-D., Chapple, C., & Somerville, C. R. (1997). Mutants of *Arabidopsis thaliana* with altered cell wall polysaccharide composition. *Plant Journal*, *12*, 335–345.

Ryden, P., Sugimoto-Shirasu, K., Smith, A. C., Findlay, K., Reiter, W.-D., & McCann, M. C. (2003). Tensile properties of Arabidopsis cell walls depend on both a xyloglucan cross-linked microfibrillar network and rhamnogalacturonan II–borate complexes. *Plant Physiology*, *132*, 1033–1040.

Ulvskov, P., Wium, H., Bruce, D., Jørgensen, B., Qvist, K. B., Skjøt, M., et al. (2005). Biophysical consequences of remodeling the neutral side chains of rhamnogalacturonan I in tubers of transgenic potatoes. *Planta*, *220*, 609–620.

Vanzin, G. F., Madson, M., Carpita, N. C., Raikhel, N. V., Keegstra, K., & Reiter, W.-D. (2002). The *mur2* mutant of *Arabidopsis thaliana* lacks fucosylated xyloglucan because of a lesion in fucosyltransferase AtFUT1. *Proceedings of the National Academy of Sciences of the United States of America*, *99*, 3340–3345.

Vincken, J. P., Schols, H. A., Oomen, R. J. F. J., McCann, M. C., Ulvskov, P., Voragen, A. G. J., et al. (2003). If homogalacturonan were a side-chain of rhamnogalacturonan I: Implications for cell wall architecture. *Plant Physiology*, *132*, 1781–1789.

Yong, W., O'Malley, R., Link, B., Binder, B., Bleecker, A., Koch, K. E., et al. (2005). Plant cell wall genomics. *Planta*, *221*, 747–751.